International Journal of GEOMATE
(Geotechnique, Construction Materials and Environment)
ISSN: 2186-2982 (P), 2186-2990 (O), Japan
Vol. 31, Issue 144, August, 2026, pp.192-199; DOI: 10.21660/2026.144.g15184

EFFECT OF MESH RESOLUTION ON NUMERICAL SIMULATION OF SEDIMENT TRANSPORT AROUND A CYLINDRICAL BRIDGE PIER USING REEF3D

Shu Tsuyumine[1], *Tatsuya Matsuda[2], and Naoto Naito[3]

[1] Master's graduate, Department of Architecture and Civil Engineering, Toyohashi University of Technology, Japan
[2] Department of Architecture and Civil Engineering, Toyohashi University of Technology, Japan
[3] Civil and Environmental Engineering, Nagoya Institute of Technology, Japan

*Corresponding Author, Received: 01 April 2026, Revised: 18 May 2026, Accepted: 27 July 2026

ABSTRACT: Scouring around bridge foundations installed within riverbeds can significantly affect structural safety, potentially causing pier overturning, settlement, or tilting owing to river-flow-induced scour and erosion. Such structural failures can disrupt transportation networks and significantly impact people's daily lives. Understanding and accurately predicting the scouring behavior around a structure is essential for ensuring the stability of bridge foundations and preventing structural failures. In this study, the applicability of scouring assessment methods was evaluated by a reproduction analysis conducted using REEF3D, an open-source computational fluid dynamics and wave modeling framework. REEF3D facilitates high-resolution simulations of sediment transport and scour processes via optimized hydrodynamic modules depending on the flow conditions. In this study, simulations were performed using three different mesh sizes to evaluate the validity of the numerical results through comparison with model test data. The numerical simulation results successfully reproduced the general scouring tendencies around the pier, including the initiation of scour on the upstream side. Furthermore, refining the mesh size improved the agreement with the experimental values in terms of the scour depth. However, the maximum scour depth was slightly underestimated compared with the experimental results. These findings highlight the need for careful consideration of analytical conditions when numerically reproducing sediment transport phenomena observed in model tests.

Keywords: REEF3D, Bridge pier, Sediment transport, Mesh resolution

1. INTRODUCTION

Recently, severe flood events have caused significant scouring around river bridge piers, resulting in the settling and tilting of structures. Enomoto et al. [1] investigated the local scour around a bridge damaged by flooding and suggested that the widening of the bridge foundation during seismic retrofitting had increased the local scour depth. They highlighted the importance of considering changes in river flow conditions when assessing the scour risk. Takebayashi et al. [2] examined the cause of bridge pier failure and attributed it to riverbed scouring around the pier, which was induced by flooding. At the bridge site, the fine-grained riverbed material caused rapid bed degradation. Their findings indicated that pier settlement could be prevented by implementing effective erosion protection around piers, based on the expected bed lowering. Proactive countermeasures are necessary to prevent or mitigate damage to bridge structures because such failures disrupt transportation networks and seriously affect daily life. Understanding and accurately predicting the scour behavior around structures is essential for ensuring the stability of bridges, preventing structural damage, and supporting the safety and well-being of the public.

Bed-level changes around hydraulic structures have been experimentally and numerically studied owing to their importance in disaster prevention. Matsuda et al. [3] conducted physical model experiments and numerical simulations using REEF3D (Kamath et al., [4]; Ahmad et al., [5]) to elucidate the fundamental mechanisms of wave-induced scour around cylindrical structures. Numerical simulations were conducted and validated against physical model tests for a bare seabed and good reproducibility was obtained. When a monopile foundation was installed in the numerical and physical tests, the flow velocity on the seabed in the offshore and inshore directions increased on the side of the foundation perpendicular to the direction of the wave motion.

In the model test, scouring occurred at the same location and was attributed to the flow velocity. However, scouring occurred locally, underscoring the need for a detailed analysis of the associated factors. Kadono et al. [6] and Kadono [7] conducted model tests using a 1/40 scale cylindrical pier model and investigated the characteristics of local scour. Ishii et al. [8] developed a bed variation analysis method for reproducing three-dimensional sediment transport by solving three-dimensional motion equations and comprehensively evaluated the local scour on the upstream side of bridge piers.

This study aims to clarify the progression of scour around cylindrical structures induced by unidirectional flow considering the characteristics of soil materials. To this end, the open-source in computational fluid dynamics (CFD) system REEF3D was employed in river environments to enhance the accuracy of scour simulations and to tackle existing issues in numerical modeling.

Numerical simulations using REEF3D were conducted to analyze sediment dynamics by examining detailed flow features around a cylindrical structure and their effects on the riverbed. The sediment transport processes around the cylindrical structure were evaluated by comparing the topographic changes observed in the physical model tests with the simulation results obtained from three grid configurations: a 10 mm mesh, a 5 mm mesh, and a non-uniform mesh.

2. RESEARCH SIGNIFICANCE

The stability of bridge foundations is critical for maintaining reliable transportation infrastructure, as scour-induced failures can disrupt transportation networks and significantly impact daily life. Therefore, establishing accurate numerical methods for predicting local scour is essential for disaster prevention. This study evaluates the applicability of the numerical model REEF3D through a reproduction analysis of flow-induced sediment transport around cylindrical structures. By investigating the influence of the mesh resolution on reproducibility, this research provides valuable insights for improving the accuracy of scouring simulations in practical engineering applications.

3. MODEL TEST

Kadono et al, [6] and Kadono [7] conducted model tests to clarify to mechanism of scour around a cylindrical structure induced by a horizontal current. This section introduces the experimental model test.

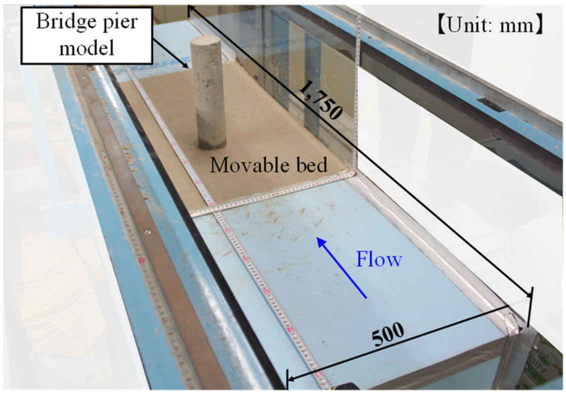

(a) Open channel flume view

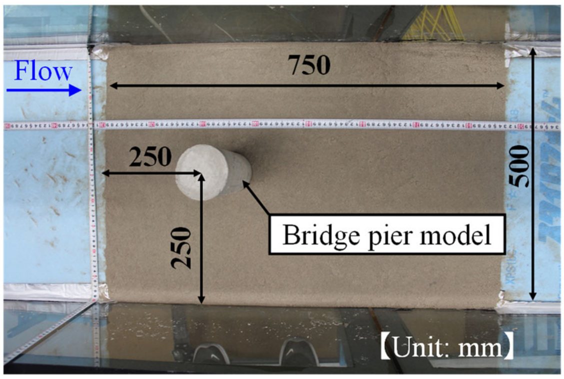

(b) Movable bed area

Fig.1. Model test flume (Adapted from [7])

An open-channel flume with a total length of 15.5 m and a width of 0.5 m was used. A 1.75 m-long section was designed to simulate a water conveyance channel (Figure 1 (a)). At the center of this section, a movable-bed zone measuring 0.5 m in width, 0.75 m in length, and 0.18 m in depth was installed (Figure 1 (b)). The movable bed consisted of No. 7 silica sand with a mean particle diameter of 0.11 mm, adjusted to a water content of approximately 18 %.

The pier model was assumed to represent an approximate geometric scale of 1/40 relative to the prototype structure. A circular mortar specimen with a diameter of 0.065 m and a height of 0.45 m was fabricated and used as the pier model. The model pier was placed at the centerline of the channel width, 0.25 m downstream from the upstream edge of the movable bed. The pier model was sufficiently embedded in the bottom soil layer to prevent deformation such as tilting during the flow experiment.

The target flow depth was set to 0.075 m, the representative flow velocity was 0.107 m/s, and the flow duration was 1800 s. The corresponding Froude number was 0.125.

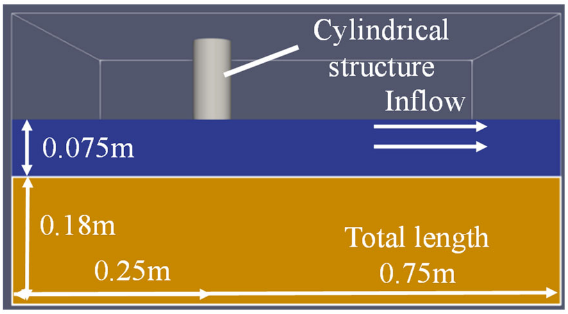

Fig.2. Region of numerical analysis: side view

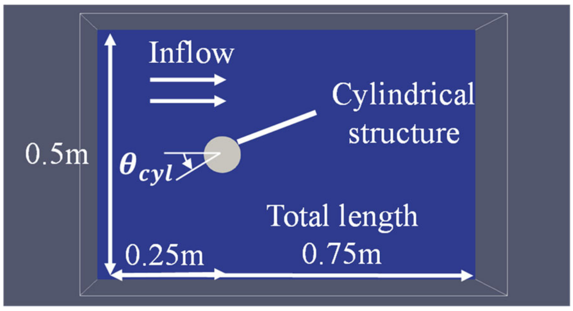

Fig.3. Region of numerical analysis: plane view

4. NUMERICAL SIMULATION METHOD

The REEF3D model is governed by the incompressible Reynolds-averaged Navier–Stokes (RANS) and continuity equations.

$$\frac{\partial u_i}{\partial x_i} = 0 \tag{1}$$

$$\frac{\partial u_i}{\partial t} + u_j \frac{\partial u_i}{\partial x_j} = -\frac{\partial P}{\partial x_i} + \frac{\partial}{\partial x_j}\left[v \left(\frac{\partial u_i}{\partial x_j} + \frac{\partial u_j}{\partial x_i} \right) - \overline{u_i u_j} \right] + g_i \tag{2}$$

Here, u, t, x, v, P, and g denote the flow velocity, time, position on the x-axis, kinematic viscosity, density of water, pressure, and gravity, respectively.

In CFD models, the fluid velocity is assumed to be sufficiently low such that the compressibility of water and air can be neglected. This allows the simplification of the flow using the RANS and continuity equations.

REEF3D, which addresses two-phase flows, uses the level-set method to capture the air–water interface. In this method, the interface between the two phases is defined as the reference surface, and the regions on either side of the interface are represented using a distance function.

The sediment transport model was used based on the flow field simulated using the hydrodynamic REEF3D model. Changes in the bed elevation were evaluated using the Exner equation, which follows

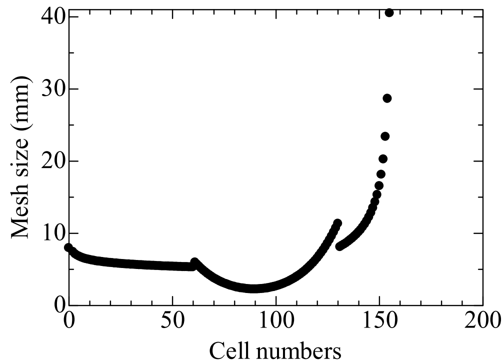

(a) Streamwise direction

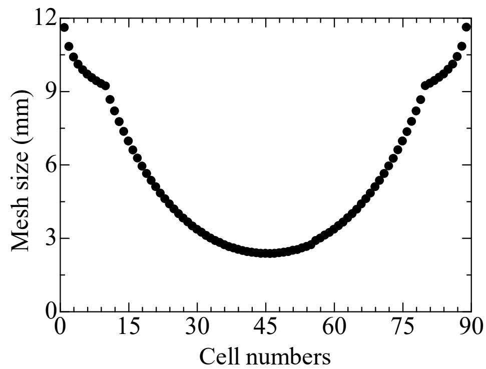

(b) Spanwise direction

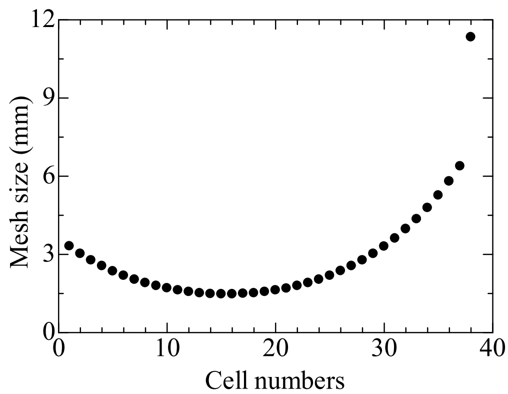

(c) Vertical direction

Fig.4. Mesh sizes in the streamwise, spanwise, and vertical directions

the conservation of sediment mass:

$$\frac{\partial z_b}{\partial t} + \frac{1}{(1-n)}\left[\frac{\partial q_{sb,x}}{\partial x} + \frac{\partial q_{sb,y}}{\partial y} \right] + E - D = 0 \tag{3}$$

Here, z denotes the bed elevation; n represents the porosity; $q_{sb,x}$ and $q_{sb,y}$ are the bedload transport rates in the x and y-directions, respectively, as

Table 1. Conditions for numerical analysis

Cylinder diameter (m)	0.065
Bed elevation (m)	0.18
Water depth (m)	0.075
Flow velocity, V (m/s)	0.107
Particle size (mm)	0.11

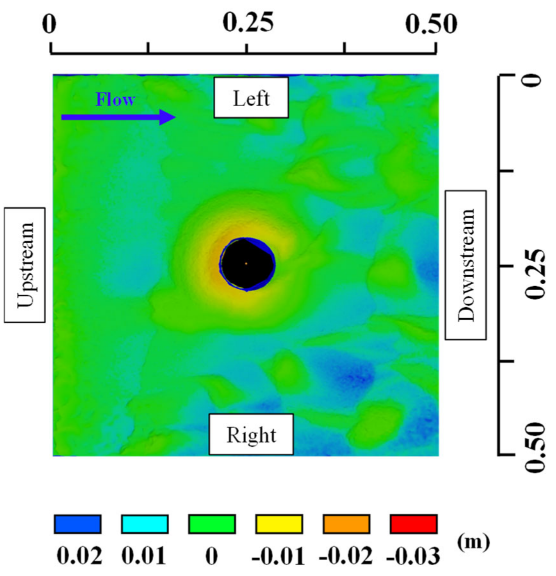

Fig.5. Sand surface profile near the cylindrical structure in the model test (Adapted from [7])

defined at the morphological time step; E is the entrainment rate from the bedload to the suspended load; and D is the settling rate from the suspended load back to the bed.

5. ANALYSIS MODEL

Figures 2 and 3 show the side and plane views of the numerical analysis, respectively. In this analysis, a computational domain with a length of 0.75 m, width of 0.5 m, and height of 0.4 m was defined, and unidirectional flow was introduced from the left boundary of the domain.

The hydraulic and soil conditions were set to match the experimental parameters reported in [6] and [7], with the median grain diameter D_{50} of the movable bed set to 0.11 mm. The computational grid was constructed using three different configurations of cubic cells: 10 mm mesh, 5 mm mesh, and a non-uniform mesh. The mesh distribution of the non-uniform grid is shown in Figures 4 (a-c). The mesh sizes in the streamwise, spanwise, and vertical directions are shown in Figure 4(a-c), respectively.

6. RESULT AND DISCUSSIONS

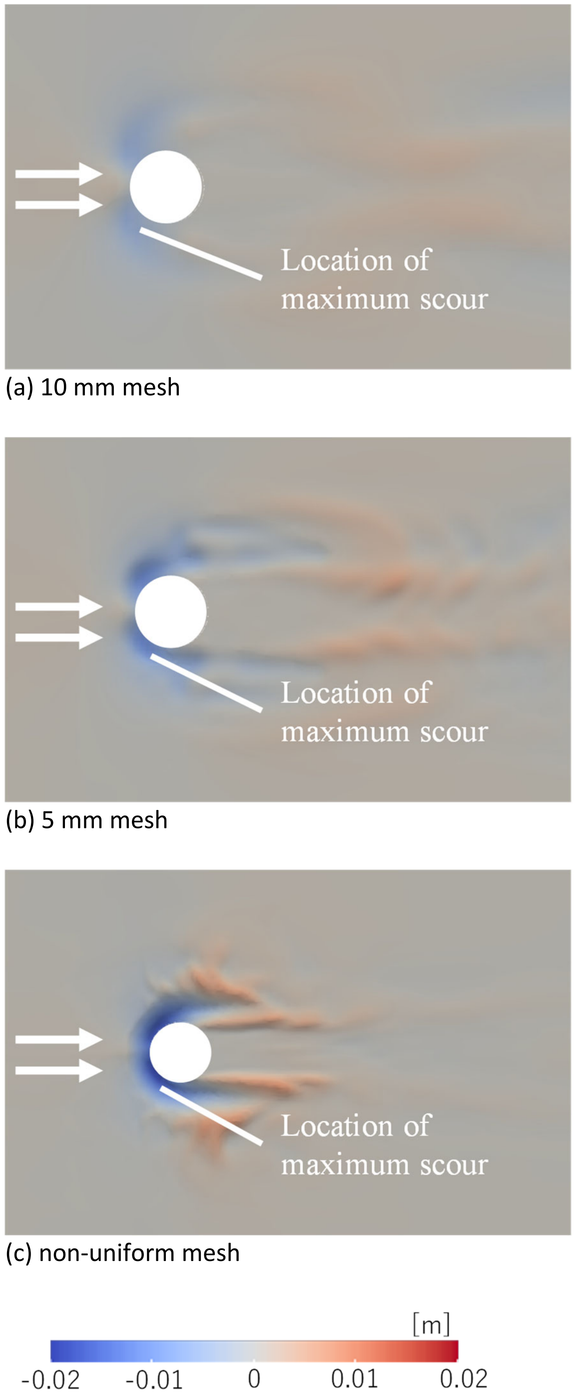

Fig.6. Sand surface profile near the cylindrical structure in the numerical analysis

6.1 Bed surface profile

Figures 5 and 6 compare the model test results with the numerical analyses performed using three mesh configurations: 5 mm, 10 mm, and non-uniform meshes.

According to Kadono [7], the model experiments demonstrated that a locally scoured, inverted

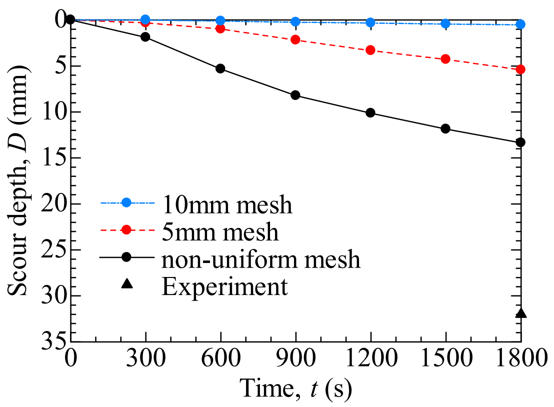

Fig.7. Scour depth around $\theta_{cyl} = 0°$

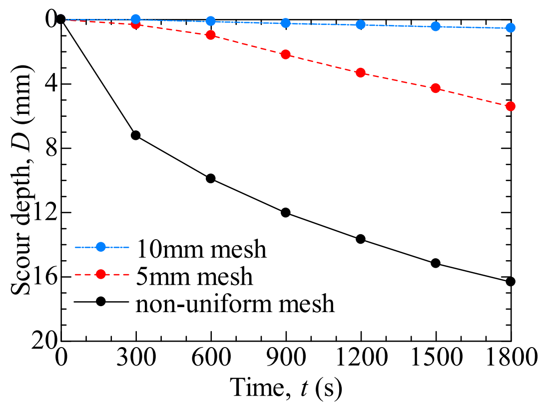

Fig.8. Maximum scour depth in the numerical analysis

conical pit formed on the upstream side of the pier model, while a depositional zone developed on the downstream side. This tendency is considered to be consistent with those reported in previous studies (Richardson and Davis [9]). In addition, in the development of local scour, observations indicated that scour initiated from the obliquely upstream side of the cylindrical specimen and then propagated toward the surrounding area along the side wall of the cylinder, eventually forming a local scour hole. This process was similar to the scour development process reported by Nakagawa and Suzuki [10] and the experimental observations of Umeda et al. [11].

In both the model test and all numerical results, scour initiation occurred in the vicinity of θ_{cyl} = 45° the upstream side of the cylinder. Furthermore, as the mesh resolution was refined, the scouring progressed towardθ_{cyl} = 0°, yielding results closer to the model test. In the uniform mesh cases, sediment deposition was observed behind the cylinder, exhibiting the same tendency as the experimental results.

6.2 Maximum scour depth

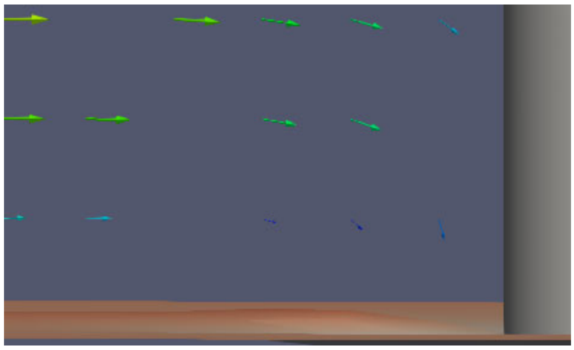

(a) 10 mm mesh

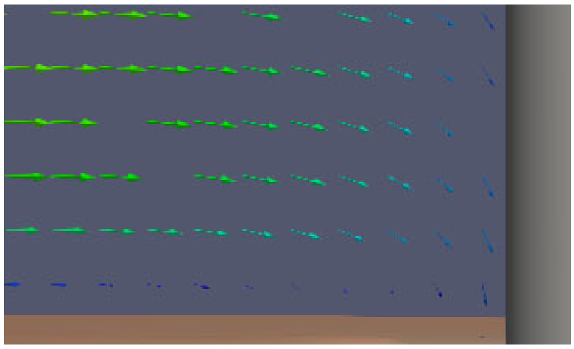

(b) 5 mm mesh

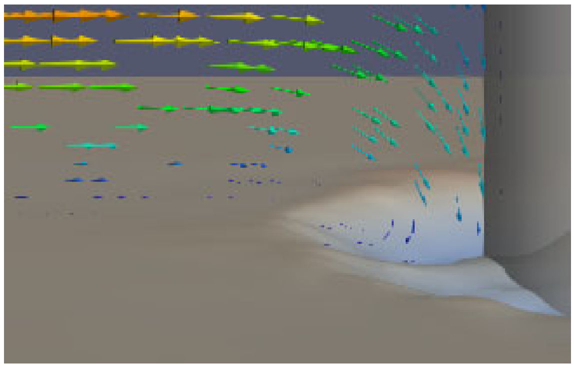

(c) Non-uniform mesh

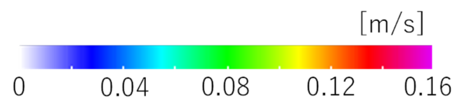

Fig.9. Flow velocity vectors in front of the cylindrical structure for each analysis

Figure 7 shows the scour depth around the cylindrical structure θ_{cyl} = 0°, and Figure 8 presents a comparison graph of the maximum scour depth. In all numerical results, the greatest scour depth was observed around θ_{cyl} = 45°, reaching approximately 16 mm. Furthermore, the maximum scour depth increased as the mesh resolution was refined. In contrast, in the model test, the scour depth was notable around θ_{cyl} = 0°, with a maximum value of 32 mm. Since the maximum scour depth around θ_{cyl}

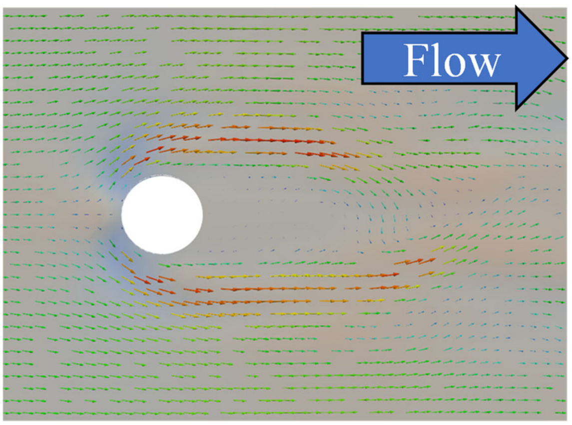

(a) 10 mm mesh

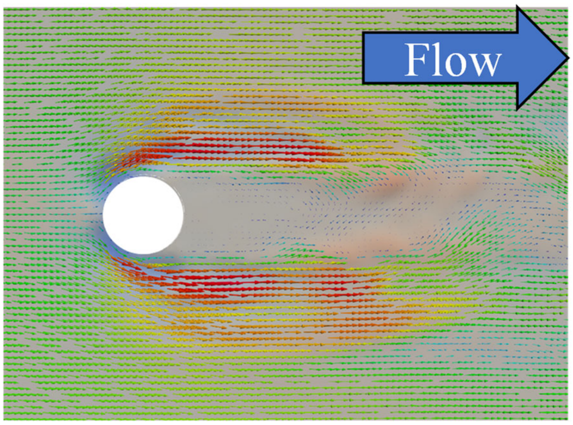

(b) 5 mm mesh

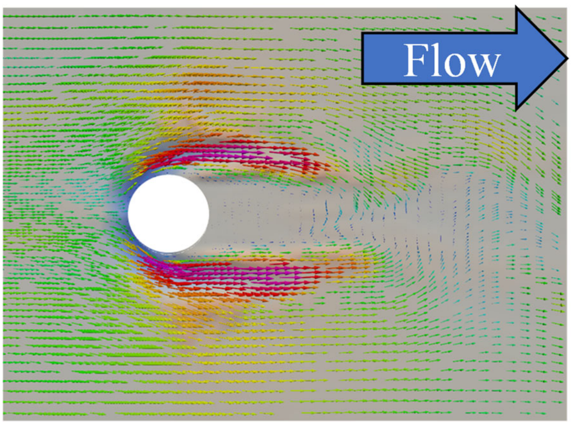

(c) Non-uniform mesh

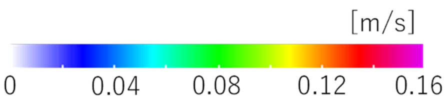

Fig.10. Near-bed velocity vectors at a height of 0.01 m from the initial bed level

= 0° in the numerical analysis was approximately 14 mm, the model test and numerical analysis exhibited different scour patterns.

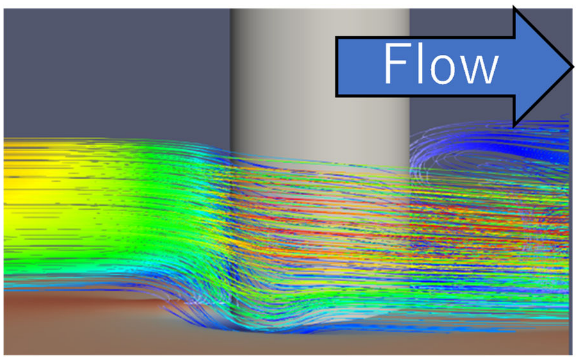

(a) 10 mm mesh

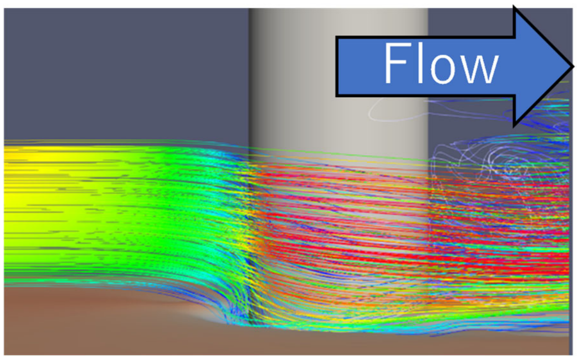

(b) 5 mm mesh

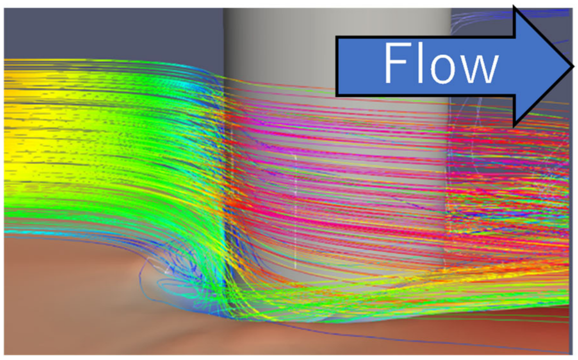

(c) Non-uniform mesh

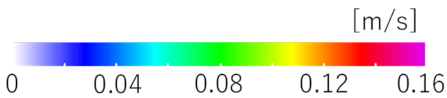

Fig.11. Streamlines around the cylindrical structure

6.3 Flow field and shear stress

Figure 9 shows the flow velocity vectors in front of the cylindrical structure for each analysis. Figure 10 presents the near-bed velocity vectors at a height of 0.01 m from the initial bed level, and Figure 11 displays the streamlines around the cylindrical structure.

A comparison of the velocity vectors in front of the pier (Figure 9) reveals flow features such as downward flow and horseshoe-vortex-like structures in the non-uniform mesh case. These flow structures are considered to influence the differences in the scour shape at the front of the pier.

Furthermore, a comparison of the near-bed velocity vectors (Figure 10) and streamlines (Figure 11) reveals that decreasing the mesh size results in increased velocity vectors from the side to the rear of the cylinder.

This increase in the flow velocity is considered a contributing factor to the increased scour depth. Thus, refining the mesh enhances the reproducibility of the flow field, thereby yielding results that closely resemble those of the physical model test.

7. CONCLUSION

The scour phenomenon around a cylindrical structure under unidirectional flow was analyzed using REEF3D to investigate the flow characteristics and sediment dynamics. The following conclusions were drawn:

- The model experiments demonstrated that a locally scoured, inverted conical pit formed on the upstream side of the pier model. In addition, in the development process of local scour, observations indicated that the scour initiated from the obliquely upstream side of the cylindrical specimen and then propagated toward the surrounding area along the side wall of the cylinder, eventually forming a local scour hole. Scouring occurred at $\boldsymbol{\theta_{cyl}}$=45° on both sides of the cylinder in the numerical analysis. In the model test, scour holes were formed around the entire circumference of the cylinder, whereas they were primarily observed between $\boldsymbol{\theta_{cyl}}$ = 45° and $\boldsymbol{\theta_{cyl}}$ = 90° in the numerical analysis.
- Sediment deposition occurred near $\boldsymbol{\theta_{cyl}}$ = 180°, in the downstream side of the cylinder, which was similar to the experimental observations.
- The maximum scour depth in the model test was approximately 32 mm, whereas the numerical analysis underestimated it by approximately 16 mm.
- The finer mesh enabled more detailed flow simulation near the structure and yielded results closer to the experimental observations.
- The bed configuration was successfully reproduced using the open-source code REEF3D.

These results highlight the need for careful consideration of the analytical conditions when numerically reproducing sediment transport phenomena observed in physical model tests. Further investigations are required to improve the accuracy of the current reproduction and enhance scour prediction methodologies. Additionally, incorporating more complex turbulence models and refining sediment transport mechanisms could improve the numerical accuracy.

Future studies will focus on optimizing computational parameters and validating the model under various flow conditions to enhance agreement with experimental results. Furthermore, to improve the reproducibility of hydrodynamics and sediment transport, the influence of modifying the computational model and sediment parameters, such as the Shields number, on the analysis accuracy will be investigated.

8. ACKNOWLEDGEMENTS

The authors acknowledge Dr. Takuya Kadono (National Institute of Technology, Anan College) for providing experimental information and for valuable comments on the interpretation of the results. This study was supported by JSPS KAKENHI Grant Numbers 25K01321, 25K22113, and 20K14824.

9. REFERENCES

[1] Enomoto T., Horikoshi K., Ishikawa K., Mori H., Takahashi A., Unno T., Watanabe K., Levee damage and bridge by 2019 typhoon Hagibis in Kanto Region, Japan, Soils and Foundations, Vol. 61, Issue 2, 2021, pp. 566–585. (in Japanese)

[2] Takebayashi H., Fujita M., Bridge Collapse in Mutsu, Aomori Prefecture, Japan in 2021, Flood Risk Management, Vol. 18, Issue 1, 2025, e70025. (in Japanese)

[3] Matsuda T., Miura K., Naito N., Shirakura D., A numerical simulation of local scour process due to waves around monopile foundation using REEF3D, Geomate, Vol. 27, No. 120, 2024, pp. 1-8.

[4] Kamath A., Alagan Chella M., Bihs H., Arntsen Ø.A., CFD Investigations into Wave Forces and Flow around Three Cylinders Placed in Different Configurations, Engineering Applications of Computational Fluid Mechanics, Vol. 9, No. 1, 2015, pp. 343-354.

[5] Ahmad N., Bihs H., Myrhaug D., Kamath A., Arntsen Ø.A., Three-Dimensional Numerical Modelling of Wave-Induced Scour Around Piles in a Side-by-Side Arrangement, Coastal Engineering, Vol. 138, 2018, pp. 132-151.

[6] Kadono T., Kato S., Okazaki S., Matsui T., Kajitani Y., Ishizuka M., Yoshida H., Effects of Dynamical Change in Water Level on Local Scouring around Bridge Piers Based on In-Situ Experiments, Water, Vol. 13, Issue 21, 2021, 3015.

[7] Kadono T., Damage Risk Potential Assessment and Maintenance Management of Bridge Piers Due to Local Scour, Doctoral dissertation, Kagawa University, 2022, pp.1-155. (in Japanese)

[8] Ishii H., Murotani K., Nakade K., Numerical Model of Local Scour around Pier Based on the 3D Analysis of Sediment Particle Motion, Journal of Japan Society of Civil Engineers Ser B1 (Hydraulic Engineering), Vol. 78, No. 2, 2022, pp. I_1201 - I_1206. (in Japanese)

[9] Richardson E. V., Davis S. R., Evaluating Scour at Bridges; Federal Highway Administration, Office of Bridge Technology (National Highway Institute, Washington, DC, USA), 2001.

[10] Nakagawa H. and Suzuki K., Enchu kyokyaku shuhen no nagare to kyokusho senkutsu nit suite [Flow around a circular bridge pier and local scour], Suiri Kouenkai Kouenshu, JSCE, Vol.16, 1972, pp. 31-36. (in Japanese)

[11] Umeda S., Yamazaki T. and Yuhi M., Effects of foundation location on scour process around a cylindrical bridge pier, Annual journal of hydraulic engineering, JSCE, Vol. 54, 2010, pp. 835-840. (in Japanese)